

## Observation of quantum beats in the $6D_{3/2} \rightarrow 5P_{1/2}$ transition in $^{85}\text{Rb}$

W. A. van Wijngaarden, K. D. Bonin, and W. Happer

*Department of Physics, Princeton University, Princeton, New Jersey 08544*

(Received 1 May 1985; revised manuscript received 23 September 1985)

Quantum beats due to the hyperfine interaction were observed in the  $6D_{3/2} \rightarrow 5P_{1/2}$  transition in  $^{85}\text{Rb}$ . Good agreement with theory was obtained, allowing determination of the values for the magnetic dipole ( $a = 2.32 \pm 0.06$  MHz) and electric quadrupole ( $b = 1.62 \pm 0.06$  MHz) hyperfine constants for the upper state.

### I. INTRODUCTION

The hyperfine interaction for the  $6D_{3/2}$  state of rubidium has been studied by Svanberg *et al.*<sup>1-4</sup> using a level-crossing experiment. An alternative method for measuring the magnetic dipole and electric quadrupole hyperfine constants, is that using quantum beats.<sup>5-11</sup> These signals have more intricate structure than those obtained from the level-crossing experiments and hence yield more precise information.

In this experiment the theoretically predicted signals were fit to the experimental data. It was found that the magnitude of the observed beats was nearly half that predicted. Since the hyperfine coupling constants are unrelated to the beat sizes, we took this factor of 2 into account to obtain close agreement between the fitted and observed signals. We believe the resulting value for the electric quadrupole constant is substantially more accurate than that found previously.

### II. THEORY

#### A. Excitation of rubidium

Rubidium atoms were excited from the  $5S_{1/2}$  ground state to the  $6D_{3/2}$  state as shown in Fig. 1, by linearly polarized light from a pulsed dye laser (pulse duration is 5 nsec). Taking the laser polarization direction as the quantization axis, the allowed transitions are governed by the selection rule  $\Delta m_J = 0$ , where  $m_J$ , the azimuthal quantum number, is a good quantum number if the hyperfine splitting is ignored. Hence, only the  $m_J = \pm \frac{1}{2}$  sublevels of the  $6D_{3/2}$  state were populated. Here we have assumed that the  $m_J = \pm \frac{1}{2}$  sublevels of the ground state are initially in equilibrium such that they have equal populations. In addition we have assumed that the laser excites the  $m_J = \pm \frac{1}{2}$  sublevels of the  $6D_{3/2}$  state equally. For a two-photon excitation, this holds when the laser linewidth exceeds the  $0.1 \text{ cm}^{-1}$  hyperfine energy splitting of the ground state. In our case, the nominal laser linewidths with and without insertion of an etalon are  $0.07$  and  $0.5 \text{ cm}^{-1}$ , respectively. However, no difference in signal was observed when the etalon was removed from the laser cavity. Hence, the hyperfine splitting of the ground state was neglected.

#### B. Discussion of the theory

Since all but one of the rubidium electrons are in fully occupied shells, the rubidium atom can be accurately modeled as a hydrogenic system where only the single outer electron along with the nucleus need be considered. The Hamiltonian  $H$  is then given by

$$H = H_0 + ah\mathbf{I} \cdot \mathbf{J} + bh \frac{[3(\mathbf{I} \cdot \mathbf{J})^2 + \frac{3}{2}(\mathbf{I} \cdot \mathbf{J}) - (\mathbf{I} \cdot \mathbf{I})(\mathbf{J} \cdot \mathbf{J})]}{2I(2I-1)J(2J-1)} + \mu_B g_J \mathbf{J} \cdot \mathbf{B} + \mu_B g_I \mathbf{I} \cdot \mathbf{B} \quad (1)$$

The first term  $H_0$  represents the Coulomb and fine-structure interactions. The next two terms are the magnetic dipole and electric quadrupole interactions that together are responsible for the hyperfine structure.  $\mathbf{I}$  and  $\mathbf{J}$  are the angular momenta of the nucleus and outer elec-

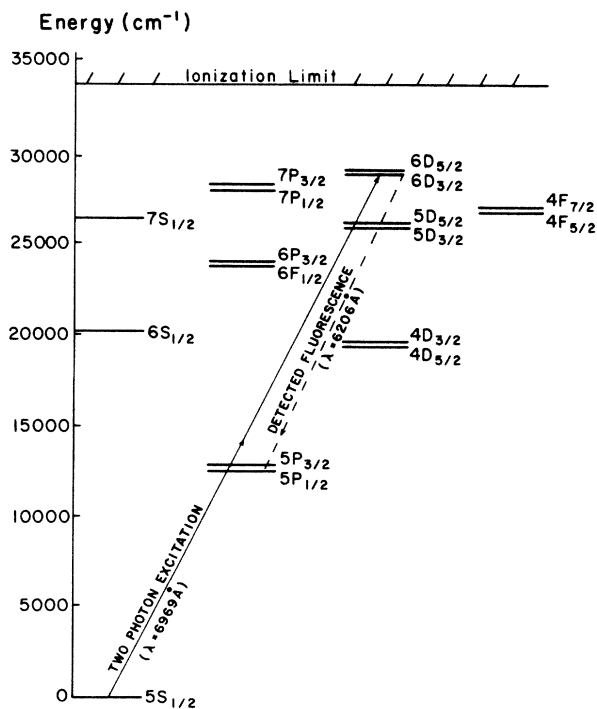


FIG. 1. Low-lying rubidium energy levels.

tron, respectively, while  $a$  and  $b$  are the hyperfine interaction constants. The last two terms represent the interaction of the electron and nucleus with an external magnetic field  $\mathbf{B}$ . The gyromagnetic ratios of the electron and nucleus are, respectively,  $g_J$  and  $g_I$  while  $\mu_B$  is the Bohr magneton.

Suppose a strong magnetic field such that  $\mathbf{I}$  and  $\mathbf{J}$  are decoupled (i.e.,  $\mu_B g_J \mathbf{J} \cdot \mathbf{B}$  is much greater than the hyperfine interaction) is applied along the polarization axis. Then our initial state is an eigenstate of the Hamiltonian. Hence, the fluorescent intensity is predicted to decay exponentially as indeed was observed.

When the earth's field is nulled away, (with our Helmholtz coil setup, residual magnetic fields were reduced to less than 10 mG) the eigenstates are the  $|JIFm_F\rangle$  states, where  $\mathbf{F}=\mathbf{J}+\mathbf{I}$  instead of the  $|Jm_JIm_I\rangle$  states. The  $|6D_{3/2}, m_J = \pm \frac{1}{2}, I, m_I\rangle$  initial states are then linear combinations of eigenstates. There-

TABLE I. Quantum beat frequencies.

$F$	$F'$	$\frac{\omega_{FF'}}{2\pi}$
4	3	$4a + 4b/5$
4	2	$7a + 7b/20$
3	2	$3a - 9b/20$
3	1	$5a - 5b/4$
2	1	$2a - 4b/5$

fore interference terms in the expression for fluorescence intensity called quantum beats<sup>5-11</sup> will arise due to the hyperfine energy differences of the various eigenstates.

Detailed reviews of quantum beats have been written by Dodd and Series,<sup>7</sup> and by Haroche.<sup>8</sup> In these two references, it is shown that the theoretically predicted intensity at time  $t$ , emitted by atoms excited at times  $t=0$ , is given by the following expression:

$$I(t) = I_0 e^{-\gamma t} \left[ 1 + \frac{P_2(\cos\theta)}{4} \left[ \frac{1957}{1400} + \frac{15}{8} \cos(\omega_{43}t) + \frac{2}{5} \cos(\omega_{32}t) + \frac{7}{20} \cos(\omega_{21}t) + \frac{6}{7} \cos(\omega_{42}t) + \frac{28}{25} \cos(\omega_{31}t) \right] \right], \quad (2)$$

$I_0$  is a constant involving various factors such as the collection solid angle of the detector and  $\gamma$  equals the inverse of the excited-state lifetime. The modulation frequencies  $\omega_{FF'}$  are given in Table I while  $\theta$  is the angle between the laser polarization axis (in our case the vertical axis) and the transmission axis of the linear polaroid in front of the detector.

From Eq. (2) we see that the fluorescent intensity consists of a pure exponential decay term plus one modulated by oscillations resulting from the hyperfine interaction. We note that when vertical linearly polarized light is detected  $P_2(\theta=0)=1$ , while when horizontal linearly polarized light reaches the photomultiplier  $P_2(\theta=\pi/2)=-\frac{1}{2}$ . Hence the oscillations in the above two cases are predicted to be out of phase and have different amplitudes. Furthermore, Eq. (2) predicts that at angle  $\theta_m=54.7^\circ$  defined by  $P_2(\theta_m)=0$ , the oscillations should disappear completely. Checking whether this indeed hap-

pened, was an important consistency check of the theory and experiment.

### III. DISCUSSION OF EXPERIMENT

#### A. Apparatus and procedure

The experimental setup is shown in Fig. 2. The frequency-doubled output of a Nd:YAG (where YAG denotes yttrium aluminum garnet) laser pumped a dye laser at a 20-Hz repetition rate. The output of the latter, at a wavelength of 6969 Å, in turn excited the rubidium to the  $6D_{3/2}$  state via a two-photon excitation. Before it entered the rubidium cell, the dye-laser beam passed through a vertical linear polarizer.

The cell itself is a cylinder 10 in. in height and 1 in. in diameter made of Pyrex. It sits in an oven heated by jets of hot air. Before the cell was filled with rubidium, it was simultaneously evacuated by a diffusion pump and baked

TABLE II. Experimental data for  $6D_{3/2}$  state of  $^{85}\text{Rb}$ .

	$ b $ (MHz)	$ a $ (MHz)	$\tau$ (nsec)
Svanberg, Tsekeris, and Happer (Ref. 1)	$1.2 \pm 0.8^a$ $a/b > 0$	$2.28 \pm 0.06^a$	
Hogervorst and Svanberg (Ref. 2)		$2.28 \pm 0.06$	
Svanberg and Tsekeris (Ref. 3)	$1.09 \pm 0.12^a$ $a/b > 0$	$2.31 \pm 0.015^a$	
Lundberg and Svanberg (Ref. 4)			$285 \pm 16$
Nikolai and Osherovich (Ref. 14)			$294 \pm 12$
Tsekeris <sup>b</sup> (theoretical calculation)			215
Present work	$1.62 \pm 0.06$ $a/b > 0$	$2.32 \pm 0.06$	$254 \pm 27$

<sup>a</sup>These numbers were found by scaling data taken for  $^{87}\text{Rb}$ .

<sup>b</sup>Private communication.

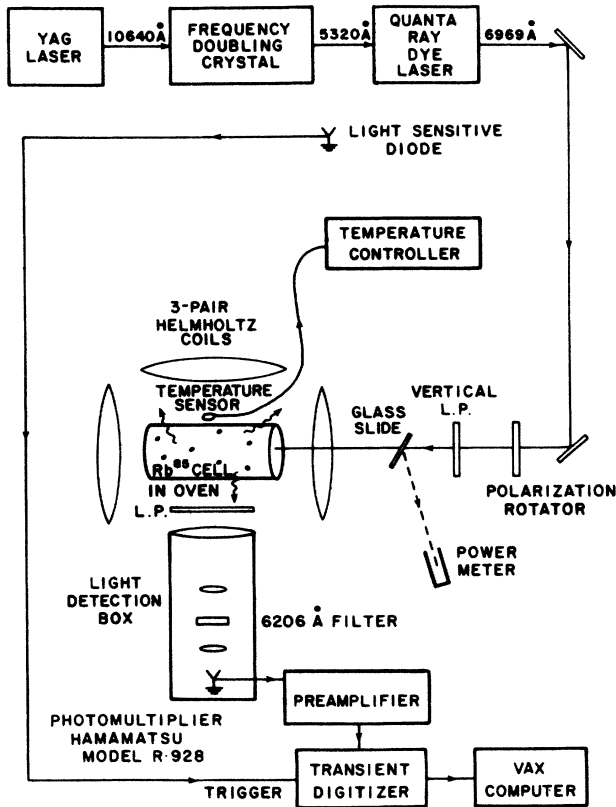


FIG. 2. Experimental apparatus.

overnight at several hundred degrees centigrade to remove impurities.

Fluorescent light was detected in the direction transverse to both the laser propagation and polarization directions. The detected light first passed through a linear polarizer and was then directed by two lenses nearly perpendicularly through an interference filter before finally being focused onto a photomultiplier. The photomultiplier was operated at sufficiently low voltages to avoid saturation. Dark current and other sources of background noise were completely negligible. The output signal was processed through a fast linear preamplifier before being put into a transient digitizer.

The transient digitizer was triggered by a fast light-

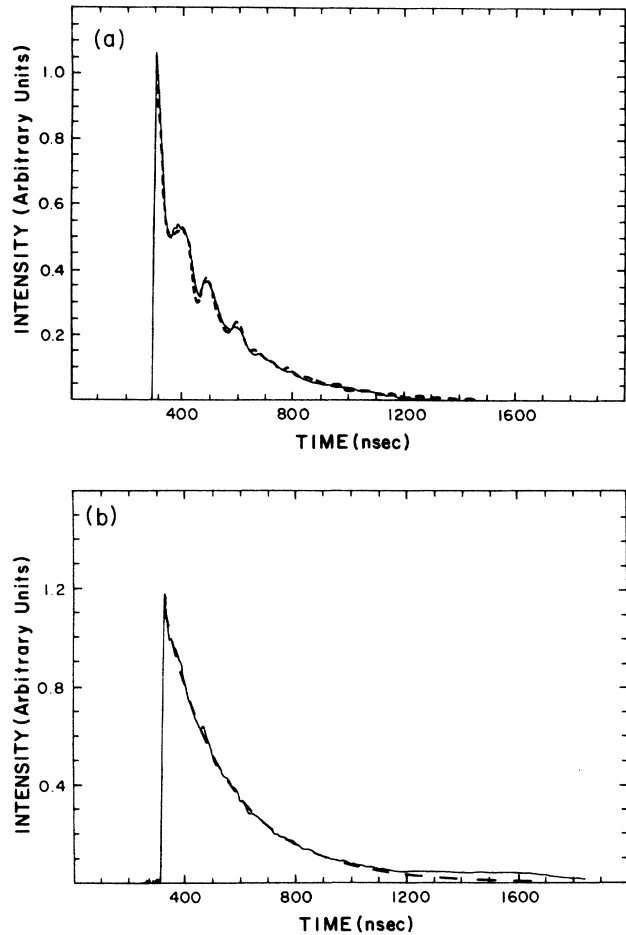


FIG. 3. Samples of experimental data. (a) This data (solid curve) were taken while a vertical linear polarizer was in front of the detector. The dashed curve is the best theoretical fit. (b) Signal when  $\theta = 54.7^\circ$ . Again the solid line is the actual data while the dashed curve is the best theoretical fit.

sensitive diode that outputs a signal at the beginning of each laser shot. The digitizer converted the analog input signal into 1024 digital channels each representing a 2 nsec time interval. Typically for a single run, data from several hundred laser pulses were additively accumulated in the instrument.

Data from each run were transmitted to a VAX computer for analysis. Using a least-squares routine, the following curve was fitted to the data:

$$S(t) = S_0 e^{-\gamma t} \left[ K + \frac{P_2(\cos\theta)}{4} \left[ \frac{1957}{1400} + \frac{15}{8} \cos(\omega_{43}t) + \frac{2}{5} \cos(\omega_{32}t) + \frac{7}{20} \cos(\omega_{21}t) + \frac{6}{7} \cos(\omega_{42}t) + \frac{28}{25} \cos(\omega_{31}t) \right] \right], \quad (3)$$

where  $S_0$  is a free parameter. Note that with the exception of  $K$ , Eq. (3) has the same form as Eq. (2).  $K$  was found from experiment to be roughly equal to 2, indicating that the oscillation amplitude was half as large as

predicted. Possible reasons for this will be given later. However, since  $K$  has no bearing on the oscillation period, it should not affect the values obtained for  $a$  and  $b$ .

## B. Results

Two of the many sets of data together with the theoretical fits are shown in Fig. 3. The oscillations disappear when  $\theta = 54.7^\circ$ , as is shown in Fig. 3(b). Also the two signals obtained using vertical and horizontal linear polarizers in front of the detector were observed to be out of phase.

The values of the fitted parameters found by averaging the results of dozens of separate runs are recorded in Table II. The error bars are equal to one standard deviation of the best-fit parameters about their mean values. In averaging the data, we have assumed the noise to be purely statistical since no systematic variation of  $\tau$  ( $\tau = \gamma^{-1}$ ),  $a$ , or  $b$  with cell temperature or laser energy was found. The cell temperature was varied from  $75^\circ\text{C}$  to  $135^\circ\text{C}$  corresponding to rubidium densities of  $10^{12}$ – $4.5 \times 10^{13}$  atoms/cm<sup>3</sup> while the laser pulse energy was varied between 1 and 8 mJ.

## C. Discussion of the observed magnitude of the quantum beats

The result that  $K \simeq 2$  means the oscillation amplitude is about half that predicted by theory. To gain insight into this discrepancy, consider the case where a strong magnetic field  $\mathbf{B}$  is applied along the axis of laser polarization. By strong we mean a field such that  $g_J \mu_B \mathbf{J} \cdot \mathbf{B}$  is much greater than hyperfine interaction. Recalling that  $g_J \gg g_I$ , we note that the Hamiltonian reduces to:

$$H = H_0 + g_J \mu_B \mathbf{J} \cdot \mathbf{B}.$$

Hence, in the regime of a strong magnetic field, effects due to  $\mathbf{I}$  are negligible.

Formally, one can obtain an expression for the fluorescence in this high field limiting case from Eq. (3) by letting all frequencies  $\omega_{FF'}$  go to zero. Then

$$S(t) = S_0 e^{-\gamma t} [K + P_2(\cos\theta)].$$

Hence the ratio  $R$  of vertical to horizontal linearly polarized fluorescence is predicted to be the following:

$$\begin{aligned} R &= \frac{S(\theta=0)}{S(\theta=\pi/2)} \\ &= \frac{2(1+K)}{-1+2K}. \end{aligned}$$

Note that  $R = 4$  when the theoretically predicted value  $K = 1$  is substituted in the preceding expression.<sup>12</sup>

It was found that the observed ratio depended strongly on the pulse energy of the excitation laser. At energies of 1–8 mJ, the observed ratio  $R$  corrected for the finite solid angle of our light detection apparatus was only about 2 which is consistent with the result  $K \simeq 2$ . At energies of about 100  $\mu\text{J}$ , however, the ratio was found to be nearly 4.0. Unfortunately, the fluorescent signals resulting from these low excitation laser energies are small and are quite noisy due to shot noise. For this reason the quantum beat

data were taken at the higher excitation laser energies of 1–8 mJ.

Before presenting a possible explanation for the energy dependence of the ratio, let us examine it more closely. The allowed electric dipole decays of the excited state ( $6D_{3/2}$ ) to the  $5P_{1/2}$  state obey the selection rule  $\Delta m_J = 0, \pm 1$ . A  $\Delta m_J = 0$  transition produces a photon that is linearly polarized in the  $z$  direction while a  $\Delta m_J = \pm 1$  transition produces a circularly polarized photon having angular momentum component  $\pm 1$  along the  $z$  axis. A circularly polarized photon will be detected when a horizontal linear polarizer is in front of our photomultiplier, but not when the former is replaced by a vertical linear polarizer. Hence, the ratio  $R$  is a measure of the amount of  $\Delta m_J = 0$  transitions compared to the number of  $\Delta m_J = \pm 1$  transitions occurring. Therefore, the observation that the ratio is less than predicted indicates that there are more  $\Delta m_J = \pm 1$  decays than expected. This could happen if the  $m_J = \pm \frac{3}{2}$  sublevels of the  $6D_{3/2}$  state are somehow initially populated.

Let us now reconsider the initial two-photon laser excitation. This populates the  $6D_{3/2}$  state while other lower-lying excited states remain empty. Hence a population inversion exists that could result in lasing action.<sup>13</sup> Indeed, the stimulated emission cross section  $\sigma_{ef}$  estimated using the dipole sum rule

$$\int_0^\infty \sigma_{ef}(\nu) d\nu = \pi r_e c f_{fe} \frac{[J_f]}{[J_e]}$$

( $[J_f] = 2J_f + 1$ , and  $J_f$  is the electron angular momentum of state  $f$ ,  $r_e$  is the classical electron radius, and  $f_{fe}$  is the absorption oscillator strength for the transition  $f \rightarrow e$ ), and assuming a Lorentzian line shape, is  $8 \times 10^{-9} \text{ cm}^2$  for the  $6D_{3/2} \rightarrow 7P_{1/2}$  transition. Unfortunately, direct observation of these lasing transitions is impossible since their wavelengths ( $\simeq 12 \mu\text{m}$ ) exceed the transmission limit of Pyrex. If lasing occurs, an atom in the  $6D_{3/2}$  state could undergo stimulated emission to a lower state, followed by an absorption of a laser photon such that it fills a  $m_J = \pm \frac{3}{2}$  sublevel of the  $6D_{3/2}$  state. Hence as the pump laser power increases, so should the population of the  $m_J = \pm \frac{3}{2}$  sublevels. This in turn will cause the ratio  $R$  to be lower than expected.

## IV. CONCLUSIONS

As shown in Table II, the resulting data compares well with earlier work except for the hyperfine constant  $b$ , which differs from that found in the most recent paper of Lundberg and Svanberg. The latter employed a level crossing experiment to measure the absolute values of  $a$  and  $b$  for  $^{87}\text{Rb}$ . In the case of  $^{85}\text{Rb}$ , however, the quadrupole constant is about twice that for  $^{87}\text{Rb}$ . Hence in our experiment,  $b$  should be easier to measure. Furthermore, our technique places tighter constraints on the fitted parameters since the quantum beat decay curves have more intricate structure than the level crossing signals. The quoted value of  $b$  is the average of data from 28 runs. It was found to be independent of systematic changes such as laser energy, cell temperature, and the type of linearly polarized fluorescence detected. The quantum beat technique has the advantage of not needing any external mag-

netic fields. Like a level-crossing experiment however, it permits only the determination of the magnitude and relative sign of the  $a$  and  $b$  constants since the intensity  $I(t)$  given by Eq. (2) is unchanged when both  $a$  and  $b$  change sign. The only restrictions on the quantum beat method are that the hyperfine coupling times be less than the excited-state lifetime and greater than the excitation pulse duration. This method should be suitable for accurately determining the  $a$  and  $b$  constants for several states in each of the alkali elements.

#### ACKNOWLEDGMENTS

The authors are very grateful to Professor Bob Austin for the use of his transient digitizer and Wuwell Liao for explaining some of the idiosyncrasies of the VAX. This work was supported by Lawrence Livermore National Laboratory Subcontract No. 3181505. One of us (W.v.W.) would like to thank the Canadian National Science and Engineering Research Council for financial support.

<sup>1</sup>S. Svanberg, P. Tsekeris, and W. Happer, *Phys. Rev. Lett.* **30**, 817 (1973).

<sup>2</sup>W. Hogervorst and S. Svanberg, *Phys. Scr.* **12**, 67 (1974).

<sup>3</sup>S. Svanberg and P. Tsekeris, *Phys. Rev. A* **11**, 1125 (1975).

<sup>4</sup>H. Lundberg and S. Svanberg, *Phys. Lett.* **56A**, 31 (1976).

<sup>5</sup>G. W. Series, *Physica* **33**, 138 (1967).

<sup>6</sup>J. S. Deech, R. Luypaert, and G. W. Series, *J. Phys. B* **8**, 1406 (1975).

<sup>7</sup>J. N. Dodd and G. W. Series, *Physics of Atoms and Molecules* (Plenum, New York, 1978), pp. 639–677.

<sup>8</sup>S. Haroche, *High Resolution Laser Spectroscopy* (Springer, New York, 1976), pp. 253–313.

<sup>9</sup>P. Schenck, R. C. Hilborn, and H. Metcalf, *Phys. Rev. Lett.* **31**, 189 (1973).

<sup>10</sup>A. Corney, *Atomic and Laser Spectroscopy* (Clarendon, Ox-

ford, 1977), pp. 661–741.

<sup>11</sup>M. Glodz and M. Krainska-Miszczak, *J. Phys. B* **18**, 1515 (1985).

<sup>12</sup>This result can be derived straightforwardly by considering the allowed  $\Delta m_J = 0, \pm 1$  transitions from the  $6D_{3/2}$  to the  $5P_{1/2}$  state as the result of the vertical or circular oscillation of a charge along or about the  $z$  axis. Using the classical dipole radiation pattern and the relative strengths of the transitions, one can confirm that  $R = 4$  when only the  $m_J = \pm \frac{1}{2}$  sublevels of the  $6D_{3/2}$  state are populated.

<sup>13</sup>M. S. Malcuit, D. J. Gauthier, and R. W. Boyd, *Phys. Rev. Lett.* **55**, 1086 (1985).

<sup>14</sup>A. Ya Nikolaich and A. L. Osherovich, *Vestn. Leningr. Univ., Fiz., Khim* **2**, 44 (1976).